Ecology Letters

WILEY

ECOLOGY LETTERS

LETTER

Seed Production and 22 Years of Climatic Changes in an Everwet Neotropical Forest

Jason Vleminckx[1] | J. Aaron Hogan[2] | Margaret R. Metz[3] | Liza S. Comita[4,5] | Simon A. Queenborough[4] | S. Joseph Wright[5] | Renato Valencia[6] | Milton Zambrano[3,6] | Nancy C. Garwood[7]

[1]Université Libre de Bruxelles, Brussels, Belgium | [2]USDA Forest Service, International Institute of Tropical Forestry, San Juan, Puerto Rico, USA | [3]Lewis & Clark College, Portland, Oregon, USA | [4]School of the Environment, Yale University, New Haven, Connecticut, USA | [5]Smithsonian Tropical Research Institute, Balboa, Republic of Panama | [6]Escuela de Ciencias Biológicas, Pontificia Universidad Católica del Ecuador, Quito, Ecuador | [7]School of Biological Sciences, Southern Illinois University, Carbondale, Illinois, USA

Correspondence: Jason Vleminckx (jason.vleminckx@ulb.be)

Received: 20 March 2024 | **Revised:** 24 September 2024 | **Accepted:** 7 October 2024

Editor: William R.L. Anderegg

Funding: This work was supported by Smithsonian Tropical Research Institute; Center for Tropical Forest Science and US National Science Foundation (DEB-0614525, DEB-1122634, DEB-1754632, DEB-1754668); University of Aarhus; British Airways; Natural History Museum, London; Natural Environment Research Council (GR9/04037); Andrew W. Mellon Foundation; Pontificia Universidad Católica del Ecuador; Government of Ecuador; Institute for Biospheric Studies, Yale University.

Keywords: climate change | everwet tropical forests | forest reproduction | relative humidity | seed production | solar irradiance | temperature | Western Amazonia

ABSTRACT

Examining the cues and drivers influencing seed production is crucial to better understand forest resilience to climate change. We explored the effects of five climatic variables on seed production over 22 years in an everwet Amazonian forest, by separating direct effects of these variables from indirect effects mediated through flower production. We observed a decline in seed production over the study period, which was primarily explained by direct effects of rising nighttime temperatures and declining average vapour pressure deficits. Higher daytime temperatures were positively related to seed output, mainly through a flower-mediated effect, while rainfall effects on seed production were more nuanced, showing either positive or negative relationships depending on the seasonal timing of rains. If these trends continue, they are likely to lead to significant changes in forest dynamics, potentially impacting both forest structure and species composition.

1 | Introduction

Tropical forests contain most of the Earth's terrestrial biodiversity and play a critical role in the global carbon cycle and regulation of climate (Valencia, Condit, et al. 2004; Pan et al. 2011; Slik et al. 2015; Mitchard 2018; Gatti et al. 2021). Efforts to better understand how climate change impacts tropical forest ecosystems are critical to their future conservation and to understanding future global carbon cycle and climate (Ometto et al. 2022). Studies from seasonal tropical forests have reported that global warming, combined with increasing water stress, is altering the physiology, growth and survival of trees, affecting forest composition and functioning (Bauman et al. 2022; Doughty et al. 2023; Kullberg et al. 2024). On the other hand, less seasonal, more humid parts of the tropics may experience contrasting changes in climate. For instance, in Western Amazonia, models predict increased cloudiness and more frequent heavy rains (Ometto et al. 2022), potentially affecting forest dynamics (Vleminckx

et al. 2023). Yet, climate change projections in the Amazon region remain uncertain (Parsons 2020; Fleischmann et al. 2023). The poor spatial and temporal resolution of in situ meteorological measurements, even where long-term plant community inventory data exist, makes linking forest responses to changes in climate and associated drivers difficult (Mendoza, Peres, and Morellato 2017; Abernethy et al. 2018; Davis et al. 2022).

So far, our understanding of the effects of climate change on tropical tree communities has largely been based on analyses of plant growth and mortality (Williamson et al. 2000; Aleixo et al. 2019), and we know very little regarding how climate relates to community-level reproduction, via the production of fruits or flowers (Wright and Calderon 2006; Cook et al. 2012; Pau et al. 2018; Vleminckx et al. 2023; Aun et al. 2024). Yet, plant regeneration, community dynamics and forest productivity are fundamentally reliant on effective pollination, seed dispersal and seed germination (Van Schaik, Terborgh, and Wright 1993). Moreover, the availability and diversity of fruit and seeds for frugivores and granivores depends on the successful production of flowers and their subsequent development (Van Schaik, Terborgh, and Wright 1993). If changing climate conditions affect the provisioning of these food resources, it could trigger bottom-up effects that cascade throughout the ecosystem, affecting both pollinators and frugivores (Butt et al. 2015).

Tropical trees typically exhibit narrow thermal niches, making them vulnerable to exceeding their photosynthetic thermal optima, which could potentially reduce carbon fixation and plant performance, including reproduction (Crous, Uddling, and De Kauwe 2022; Perez and Feeley 2018; Kullberg et al. 2024). In addition, elevated nighttime temperatures might interfere with critical temperature cues that regulate the timing of fruiting (Tutin and Fernandez 1993; Chen et al. 2018; Numata et al. 2022; Sullivan et al. 2023). Warmer nights can also reduce net carbon gains by elevating respiration (Atkin et al. 2005), which may indirectly affect reproductive processes. Additionally, moister daytime air conditions (i.e., reduced water vapour pressure deficit), when stomata are open, may reduce the water potential gradient between the leaf surface and the atmosphere. This could slow transpiration, evaporative cooling and nutrient uptake (Tibbitts 1979; Grossiord et al. 2020), especially in the wettest parts of the tropics (Lin et al. 2017), which may potentially impact reproduction. In an everwet tropical forest in Ecuador, the combination of elevated nighttime temperatures and high average relative humidity has been linked to a reduction in flower production over 18 years (Vleminckx et al. 2023). At the same time, while elevated temperatures have a negative impact on the net carbon gain of tropical plants (Sullivan et al. 2020), studies have also reported a positive influence of warmer daytime atmospheric conditions on both flower (Vleminckx et al. 2023) and seed production (Potts et al. 2020).

Light energy (i.e., photosynthetically active radiation) is another critical factor that may limit plant reproductive efforts (Wright and Van Schaik 1994; Chapman et al. 2018) and serve as a major cue to synchronise flowering and fruiting events (Wright and Calderon 2018; Sullivan et al. 2023). In central Panama, previous observations have shown a reduction of 31% in global radiative flux at the September equinox compared to the less cloudy March equinox (Windsor 1990). Light limitation may be more persistent in everwet tropical forests near the equator because of the frequent and persistent convective cloud cover of the Intertropical Convergence Zone, which reduces light penetration (Min 2004; Pau et al. 2013). Such reduced levels of solar irradiance may impact seed output indirectly—through light-limitation of flower production—or directly—especially since unripe fruits are often photosynthetically active (Blanke and Lenz 1989). Yet, a reduction of nearly 20% in mean annual irradiance levels observed in an everwet tropical forest of Ecuador between 2000 and 2018 did not have a significant impact on tree community annual flower production (Vleminckx et al. 2023).

Here, we provide the first long-term examination of how climate variation influences seed production at the community level in a hyper-diverse equatorial everwet forest in western Amazonia. We use data from 203 species collected over a 22-year period (2000–2021) to analyse the direct effect of five climate variables (irradiance, rainfall, minimum and maximum air temperature and average water vapour pressure deficit) on annual seed production, as well as their indirect impacts on annual seed production via their effects on flower production. The five climate variables are linked; irradiance, vapour pressure deficit and maximum daytime temperature increase together. We predict that seed production will correlate positively with all three. We also predict that seed production will correlate negatively with nighttime minimum temperature. Because of limited seasonal variation in water limitation and low drought frequency, we expected either no clear signal from rainfall or a weak positive association between rainfall and seed production.

2 | Methods

2.1 | Study Site

The Yasuní Research Station (ECY, 0°41'S, 76°24'W) is affiliated with the Pontificia Universidad Católica del Ecuador and is located in Yasuní National Park, in Ecuador (Figure 1). The park is situated in one of the Amazon basin's wettest areas (Funatsu et al. 2021). From 2000 to 2022, the park received annual rainfall averaging 3165 mm, with monthly averages ranging from 194 mm to 392 mm. The highest rainfall occurs in May–June, with a secondary peak in October–November (Pitman 2000; Valencia, Condit, et al. 2004). Given this rainfall regime, the park's climate is described as aseasonal (Walter, Harnickell, and Mueller-Dombois 1975) or everwet (McGregor and Niewoldt 1998) because rainfall nearly always exceeds 100 mm month^{-1}. During the same period (2000–2022), the recorded monthly minimum, mean and maximum temperatures ranged from 20.9°C to 22.0°C, 24.1°C to 25.6°C and 29.5°C to 32.1°C, respectively.

The landscape is characterised by evergreen, terra firme moist forests at an elevation of approximately 200 m above sea level, across terrain marked by moderate undulations and slopes (Berdugo et al. 2022). Forest canopy height ranges from 15 to 30 m, with emergent trees up to 50 m tall (Valencia, Condit, et al. 2004). The soils of the region predominantly consist of Andean erosional materials (Malo and Arguello 1984) with sediment deposits from lake formations and Miocene marine incursions (Hoorn et al. 2010). This geological history has fostered

FIGURE 1 | Location of the Yasuní Forest Dynamic Plot (FDP) within the bounds of Yasuní National Park (YNP; dark grey area).

speciation and led to the biological richness of the Andean Amazon (Baraloto et al. 2021).

Phenological and climatic data were gathered from the 50-ha Yasuní Forest Dynamics Plot (YFDP), which was initiated in 1995 for the purpose of mapping, identifying, measuring and tagging all trees with a diameter ≥1 cm diameter at 1.3 m above the ground (Valencia, Condit, et al. 2004, Valencia, Foster, et al. 2004). This plot contains an exceptionally diverse flora, with 1104 species of trees and shrubs recorded in 25 ha during the first survey (Valencia, Foster, et al. 2004). Notably, it includes 40 species of *Miconia* (Melastomataceae), 40 species of *Inga* (Fabaceae) and 16 species of Myristicaceae (Valencia, Foster, et al. 2004; Queenborough et al. 2007).

2.2 | Climate Data

Hourly measurements of solar irradiance ($W m^{-2}$), rainfall (mm) and temperature (°C) were collected at ECY from May 2000 through February 2012. Solar irradiance was measured using two LI-COR LI-200S pyranometers (tuned to the daylight spectrum of 400 to 1100 nm). Air temperature was measured using an LI-1400-102. Rainfall was measured using an LI-1400-106 tipping bucket and an LI-1400 data logger (all instruments from LI-COR Inc. Lincoln, NE, USA) (Garwood et al. 2023). Beginning in January 2008, relative humidity was monitored using an LI-COR 1400-04 sensor. In 2012, the monitoring system was upgraded to a CR1000 data logger (Campbell Scientific, Logan, UT, USA), along with two Vaisala HMP45C thermometers, a Rotronic HC2-S3 hygrometer, a Hydrological Services TB4 rain gauge and two LI-COR LI-200X pyranometers (also calibrated for the daylight spectrum of 400–1100 nm). This upgraded equipment provided irradiance and temperature readings every 5 min from 2012 to August 2021, while a manual gauge collected daily rainfall data throughout and until October 2021. Challenges with equipment maintenance generated gaps in meteorological data. The percentage of missing daily data from 2000 to 2021 was 23% for rainfall, 33% for temperature, 37% for irradiance and as much as 68% for relative humidity (Figures S1 and S2). No meteorological data were available for 10.5% of the days, and all meteorological variables were available for 22% of the days (Figures S3 and S4).

We imputed missing climate data with Bayesian hierarchical probabilistic matrix factorisation (BHPMF, Schrodt et al. 2015). Each climate variable was first standardised (z-score transformation) and then normalised (Box-Cox transformation). BHPMF is a machine-learning algorithm that exploits hierarchical information from structured data and uses its correlation structure to impute missing entries (Schrodt et al. 2015). We used days and months to structure the data imputation. Imputations were enhanced by integrating daily records of maximum and minimum temperature, along with average relative humidity, obtained from the Nuevo Rocafuerte meteorological station situated approximately 115 km east of the YFDP and at a similar elevation (Figure S5). This information was sourced from the Visual Crossing weather data platform (www.visualcrossing.com). The selection of these three variables from the Nuevo Rocafuerte station was based

on their relatively strong positive correlations (Pearson $r > 0.6$) with the same variables measured at YFDP. Post hoc analyses supported the effectiveness of our imputation estimates (average of 50,000 imputed values): the average standard deviation of imputed values never exceeded 0.98 on days with missing climate data, while we found strong consistency in variable correlations pre- and post-imputation (Figures S6–S8). A visual comparison of imputed and observed values across time is shown in the supplementary information (Figure S9).

Considering our predictions concerning the impact of nocturnal vs. diurnal temperatures on seed production, we analysed minimum daily temperature (hereafter, T_{MIN}) and maximum daily temperature (T_{MAX}) independently. We used average and minimum relative humidity (denoted as RH_{AVE} and RH_{MIN}, respectively) and average temperature (T_{AVE}) and T_{MAX}, to calculate, respectively, the average and daytime water Vapour Pressure Deficit (VPD_{AVE} and VPD_{DAY}). Observed maximum relative humidity (RH_{MAX}) values, reflecting nighttime air moisture saturation, were close to 100% and showed a highly skewed distribution. This, combined with the large proportion of missing values (68%), led the imputations to produce unrealistic values (i.e., higher than 100%) for nearly 26% of imputed RH_{MAX} values (not shown), which was not the case with RH_{AVE} and RH_{MIN}. Rodwell et al. (2014) pointed out similar technical difficulties when making imputations for variables approaching their theoretical maximums. Additionally, because stomata are closed at night, we do not have a prediction regarding how nighttime vapour pressure deficit would influence reproduction. Thus, we chose not to examine the effect of VPD at night on seed output.

VPD_{AVE} and VPD_{DAY} were calculated in three steps. First, we calculated the average and daytime Vapour Pressure at Saturation (VPS_{AVE} and VPS_{DAY}, respectively), based on the Tetens equation (Tetens 1930):

$$\mathrm{VPS_{AVE}} = 0.6108^{*}\mathrm{e}^{(17.27^{*}TAVE/(TAVE+237.3))} \quad (1)$$

$$\mathrm{VPS_{DAY}} = 0.6108^{*}\mathrm{e}^{(17.27^{*}TMAX/(TMAX+237.3))} \quad (2)$$

where units are degrees Celsius for T_{AVE} and T_{MAX} and kPa for VPS. We then calculated the average and daytime Observed Vapour Pressure (OVP_{AVE} and OVP_{DAY}, respectively) as follows:

$$OVP_{AVE} = VPS_{AVE}{}^{*}\left(RH_{AVE}/100\right) \quad (3)$$

$$OVP_{DAY} = VPS_{DAY}{}^{*}\left(RH_{MIN}/100\right) \quad (4)$$

Finally, VPD_{AVE} and VPD_{DAY} corresponded to the following differences:

$$VPD_{AVE} = VPS_{AVE} - OVP_{AVE} \quad (5)$$

$$VPD_{DAY} = VPS_{DAY} - OVP_{DAY} \quad (6)$$

2.3 | Seed Production Data

Following the protocol of Wright and Calderon (1995), 200 permanent traps, each measuring 0.75×0.75 m ($0.57\,m^2$) and constructed using 1-mm fibreglass wire mesh, were installed across the YFDP at a height of 0.75 m (Garwood et al. 2023). Plant reproductive parts were collected from each trap twice a month from February 2000 until March 2023 (totalling 541 completed censuses). Another 16 censuses did not occur due to political disruptions and COVID-19 (two in 2018, 12 in 2020 and two in 2022). Seeds and fruits were counted and identified to species whenever possible. If species identification was impossible, the material was collected, a unique morphospecies was assigned, and attempts were made to identify the sample against local reproductive adults and a permanent voucher collection (Valencia, Condit, et al. 2004; Garwood et al. 2023). Based on Wright and Calderon (2006), our analysis focused on fruiting species detected in a minimum of 10 of the 200 traps in at least 1 year. This approach yielded a dataset of 203 species, spanning 125 genera and 52 families. The most highly represented families included Fabaceae (19 species), Bignoniaceae (13 species), Moraceae (11 species) and Clusiaceae (10 species). The 203 species included 69 species of emergent or canopy trees, 83 climbers, 42 understory trees or shrubs and nine epiphytes. Appendix S1 lists the 203 species, along with their family and life form.

The total seed mass collected within each trap was calculated by multiplying the count of whole fruits and fruit fragments by their species-specific seed dry mass and the average seed count per fruit, based on a database of measurements of these two traits for species found in YFDP (Appendix S2). For individual seed items (complete seeds or fragments), we multiplied their counts by species-specific seed dry mass. These calculations were aggregated across all traps to provide an estimate of the total seed mass for each census period.

2.4 | Data Analysis

To calculate an estimate of total annual seed production at the community level (hereafter, SP), we first standardised census-level seed mass values for each species separately, by dividing these values by the sum of seed mass values over all censuses. Standardisation was done separately for each species so that all species were on the same zero to one scale. For each census, we summed the standardised values across species to produce census-specific, community-level seed production values. Subsequently, we identified the commencement of the community-level fruiting phenological year, a crucial step since relying on calendar years might split the annual peak of community-level seed production across 2 years. To do so, we identified the day of the year that minimises the variance of linearised dates weighted by census-specific seed production values, following the methodology described in Vleminckx et al. (2023), also explained in detail in Appendix S3. SP was then calculated as the sum of community-level seed production values across all censuses for each phenological year. Seed production values for the 16 missing censuses were imputed using automatic ARIMA fitting model based on model selection with AIC (Appendix S3). A Ljung-Box test (Ljung and Box 1978) showed a p-value reaching 0.84, indicating that the residuals were not significantly correlated and that the model was well-fitted.

We used ordinary least squares (OLS) linear models to evaluate the relationships between SP and the five climate variables (solar irradiance, rainfall, minimum and maximum temperature and average vapour pressure deficit). For each climate variable (C),

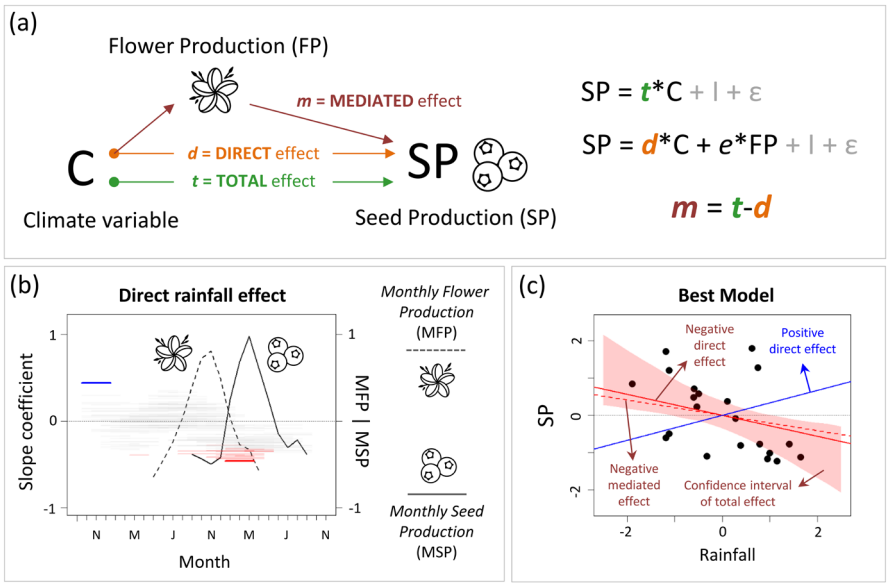

FIGURE 2 | Graphical explanation of data analysis and results presented (used for interpreting Figure 4) (a) Directed acyclic graph (DAG) showing hypothetical year-level causal relationships between any climate variable (C) and seed production (SP). The equations on the right show how the slope coefficients were calculated for: T = the total effect of C on SP in an ordinary least squares (OLS) regression; d = the direct (partial) effect of C on SP in a bivariate OLS model comprising C and the flower production (FP) as explanatory variables; and m = the effect of C on SP mediated by the effect of C on FP. I + ε = Intercept + error term of the regression model. (b) An example for the direct effect of rainfall (also shown in Figure 4f). The dashed and solid black curves represent mean monthly flower and seed production (MFP and MSP, respectively; scaled between −1 and 1 and centred on 0, right vertical axis). Only 3 months are indicated on the X-axis for clarity (N = November; M = March; J = July). The span of horizontal bars represents the range of months during which the mean rainfall value is calculated for each phenological year so that it produces the slope value indicated on the left Y-axis. Horizontal bars are coloured in blue/red if slope values are significantly positive/negative ($p \leq 0.05$; MSR test) or in grey if values are not significant. When significant, the strongest positive and negative response is emphasised with a thicker bar. (c) 95% Bayesian credibility interval (shaded area; coloured in blue/red when 95% of slope values were positive/negative) of the linear relationship between SP (vertical axis) and the direct effect of rainfall (horizontal axis). The solid and dashed lines show the slope coefficient of the direct and flower-mediated effect, respectively (coloured in blue/red if significantly positive/negative).

we calculated three OLS slope coefficients (Figure 2), quantifying: (1) the total effect of C on SP; (2) the partial direct effect of C when adding flower production in the model; and (3) the effect of C on SP mediated through flower production (Figure 2a). To facilitate interpretation, we refer to the second and third coefficients as the "direct" and "flower-mediated effect", respectively. The flower-mediated effect was quantified with the total flower production observed during each entire flowering phenological year, using the flower production data from Vleminckx et al. (2023).

To examine the period of the fruiting phenological year when the mean condition of each climate variable (C) best explains interannual variation in SP, each of the three regression slope coefficients was calculated using different seasonal time frames for C (Figure 2b). More specifically, C was calculated as the mean monthly value of a climate variable within all 222 possible ranges of 1 to 12 consecutive months over a 24-month window, starting 12 months before and ending with the current fruiting phenological year. Thus, both lagged and concurrent effects of C on SP are evaluated. Likewise, to calculate the flower-mediated effect, the 24-month window started 12 months before and ended with the current flowering phenological year.

The statistical significance of each regression slope coefficient was tested by comparing its value against a distribution of 4999 null values generated by Moran spectral randomisations (MSR, Wagner and Dray 2015). MSR is a spatially or temporally constrained randomisation method that reproduces randomised values displaying the same autocorrelated structures as the original values, which can then be used to account for type I error rate inflation risk when testing the association between two spatially or temporally autocorrelated variables (Bauman et al. 2019).

Following our predictions, we expect the slope coefficients of each of the three effects (total, direct, flower-mediated) to be negative for T_{MIN}, and positive for irradiance, T_{MAX} and VPD, with no clear prediction for rainfall. Consequently, we used one-tailed tests for the first four climate variables and a two-tailed test for rainfall, with a statistical significance threshold of 5% for all tests. Slope values were then considered significantly negative for T_{MIN} (or positive for irradiance, T_{MAX}, and VPD) if they were negative and less than (or positive and greater than) 95% of null coefficient values. Slope coefficients calculated for rainfall were considered significantly negative or positive when taking negative and positive values below or above the 2.5th and 97.5th percentiles of null values, respectively.

All analyses were performed in the *R* statistical environment v.4.4.0 (R Core Team. 2024). We provide the climate and phenological data, and R code to reproduce our analyses (including citations for R packages used), in Appendices S4–S7.

3 | Results

Over the 22-year study period, total annual community-level seed production (SP) showed an overall decreasing trend, with a pronounced drop between 2010 and 2013 (Figure 3a). Over the same period, there was a linear decrease in solar irradiance and VPD_{AVE} (Figure 3b,f), and an increase in T_{MIN} (Figure 3d). Rainfall increased slightly (Figure 3c), while maximum temperature showed no clear trend (Figure 3e).

Rainfall and T_{MIN} showed predominantly negative significant effects (both total and either direct or flower-mediated, or both) on SP (Figure 4e–l), while only positive significant effects were observed for T_{MAX} and VPD_{AVE}. (Figure 4m–t). No significant signal was observed for irradiance with the MSR testing procedure (Figure 4a–c); however, 95% of Bayesian slope estimates were positive for the total effect (Figure 4d). For rainfall, the strongest total negative effect (minimum slope coefficient = −0.69; $p = 0.001$; Figure 4e) and the strongest direct negative effect (−0.46; $p = 0.001$; Figure 4f) were obtained for rainfall between mid-December and mid-March or from the onset of the fruiting phenological year until the peak of fruiting. Additionally, the amount of rainfall during the first 3 months (mid-September to mid-December) of the preceding fruiting phenological year had a significant positive direct effect on SP (slope coefficient = 0.44; $p = 0.028$; Figure 4f). The flower-mediated effects of rainfall on SP were predominantly negative, with the strongest relationship (−0.55; $p = 0.001$) found when considering cumulative rainfall over 3 months at the beginning of the flowering season (mid-May to mid-September) (Figure 4g).

The mean nighttime temperature over an 11-month period covering approximately the entire flowering phenological year (mid-May to mid-April) had a significant negative total and direct effect on SP (−0.77 and −0.57, respectively, with $p = 0.001$; Figure 4i,j). Flower-mediated effects of nighttime temperatures were relatively weak (> −0.26) and never significant (Figure 4k). For T_{MAX}, the strongest positive total effect (0.54; $p = 0.001$; Figure 4m) was observed between mid-November and mid-March or between the peak of flowering and the peak of fruiting. We found no significant direct effect of T_{MAX} (Figure 4n). However, the mean daily temperature recorded over most of the flowering phenological year (mid-May to mid-March) had a weak, though significant positive, flower-mediated effect on SP (0.35; $p = 0.040$; Figure 4o). The strongest positive total and direct effects of VPD_{AVE} (0.84 and 0.67, respectively, with $p = 0.001$; Figure 4q,r) were found when considering mean values of this variable calculated over the 12-month and the 11-month period starting at the beginning of the flowering phenological year (May). The use of VPD_{DAY} and RH_{AVE} produced redundant but

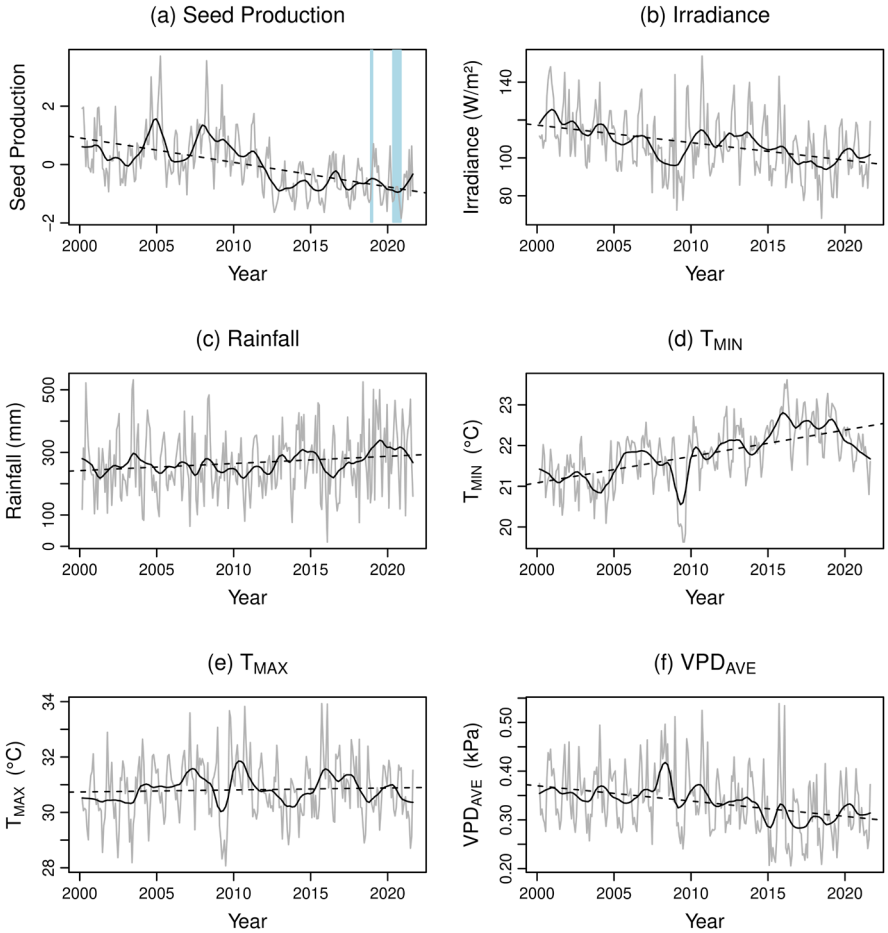

FIGURE 3 | Monthly values (grey lines), interannual trends (black lines) and linear regression trends (dotted black lines) of (a) community-level seed production and each climate variable (b–f) between February 2000 (beginning of the flower and seed sampling) and August 2021 (end of the last fruiting phenological year used in the regression analyses). The interannual trends were obtained from Seasonal-Trend Decomposition using Loess (Cleveland et al. 1990). The blue-shaded areas in panel a indicate months where seed production data was imputed using an ARIMA model fitting.

weaker signals compared to VPD_{AVE} in terms of total, direct and flower-mediated effects on SP (Figures S10–13).

Panels d, h, l, p and t in Figure 4 show the observed SP values plotted against the mean value of each climate variable calculated over the period of strongest relationship (i.e., yielding the most positive or negative slopes) for the total effect, along with regression trends for the strongest direct and flower-mediated effects.

4 | Discussion

We examined how community-level seed production responded to interannual climate variation over a 22-year period in an everwet Amazonian forest at Yasuní. Our results indicate a declining trend in community-level seed production, which was associated with a marked increase in minimum nighttime temperature and a decrease in average water vapour pressure deficit. Consistent with our expectations, these results suggest that the convergence of warmer nights and wetter atmospheric conditions occurring during the flowering phenological year, as well as at the onset and peak of the fruiting season, may have negatively impacted seed production over the past two decades. If these trends persist, tree regeneration may be depressed, with implications for community dynamics, forest biomass and potential cascading effects on tropical forest food webs. Rainfall and daytime temperature displayed more subtle interannual variation, with maximum temperature showing positive effects on seed production, while rainfall exhibited both positive and negative effects depending on the seasonal timing of rains.

4.1 | Warmer Nights and Moister Air Negatively Impact Seed Production

Total community-level annual seed production (SP) declined significantly with higher nighttime temperatures (T_{MIN}) (Figure 4i,j). This is consistent with previous findings that show how warmer nighttime temperatures increase respiratory carbon loss (Atkin et al. 2005; Slot et al. 2014; Slot and Winter 2017). These adverse effects could reduce tree and whole-forest reproductive output, if resource allocation to reproduction remains unchanged as temperature increases. Elevated nighttime temperatures may also affect seed productivity via disruption of species-specific cues for fruiting onset, fruit maturation and seed viability (Tutin and Fernandez 1993; Chen et al. 2018). Such disruptions could potentially result in asynchronous fruiting events within plant populations, potentially decreasing fruit availability to dispersers, and consequently impacting whole forest regeneration.

The decline in vapour pressure deficit over the study period (Figure 3f) likely led to a progressive reduction in transpiration capacity and evaporative cooling, which may have slowed nutrient uptake through tree xylem. These physiological changes could have adversely affected seed production, as indicated by the strong positive relationship between VPD_{AVE} and seed production (Figure 4t). It is also possible that reduced convective cooling of plants occurs due to denser cloud cover, as mean annual irradiance was strongly negatively correlated to atmospheric relative humidity (r-Pearson = −0.81; Figure S6). The negative effects of T_{MIN} and the positive effects of VPD_{AVE} were predominantly direct (Figure 4j,r) and not significantly mediated by climate-driven influences of these variables on flower production (Figure 4k,s).

4.2 | Enhanced Seed Production With Higher Daytime Temperature Prior to the Peak of Fruiting

Higher mean daytime temperatures during the onset and peak of the fruiting season were associated with greater seed production (Figure 4m,o), a pattern that was partly mediated by a positive influence of warmer days on flower production (Figure 4o). These observations are not consistent with the conclusions of a pan-tropical study, which found that elevated daytime temperatures lead to reduced net carbon fixation by plants, with no clear influence of nighttime temperatures (Sullivan et al. 2020). Although that study did not examine seed production, it underlines the need to better contextualise climate change studies depending on forest seasonality. Unlike more seasonal parts of Amazonia, tropical everwet forests like Yasuní are experiencing an increase in cloud cover (Ometto et al. 2022). The presence of more persistent and denser clouds may keep daytime temperatures below species' thermal acclimation limit. Under these conditions, a modest increase in temperature could promote seed production, by catalysing metabolic functions essential for the development of reproductive organs, coupled with an increase in the rate of litter decomposition that could facilitate nutrient recycling and indirectly foster reproduction (Pau et al. 2013). Nevertheless, one might also consider the 13.5% increase in atmospheric CO_2 concentration observed during the study period (https://keelingcurve.ucsd.edu/), which may have partly compensated for the effect of reduced solar inputs.

4.3 | Rainfall Increases or Decreases Seed Production Depending on Its Seasonal Timing

The amount of rainfall during the first 3 months of the preceding fruiting phenological year (mid-September to mid-December) showed a significant positive direct effect on SP (Figure 4f). This lagged effect suggests that water availability may limit SP during a time that overlaps with a period of the year that is, on average, relatively less humid (August to February; Garwood et al. 2023). It is also possible that reproductive cues are indirectly associated with the amount of rainfall from September to December (period of strongest positive effect). Future research is needed to better understand how seasonal variation in plant water status relates to the timing of flower and fruit production in everwet tropical forests.

Increased precipitation prior to and during peak fruiting (December to April) was associated with a direct, adverse impact on SP (Figure 4e,f). Given that irradiance showed no significant positive effect on SP during that period, we may discount the possibility that enhanced cloudiness, presumably related with increased rainfall during the onset of the fruiting season (r-Pearson correlation between rainfall and irradiance during the December–April period = −0.46; not shown), induces an energy-limitation for SP. In

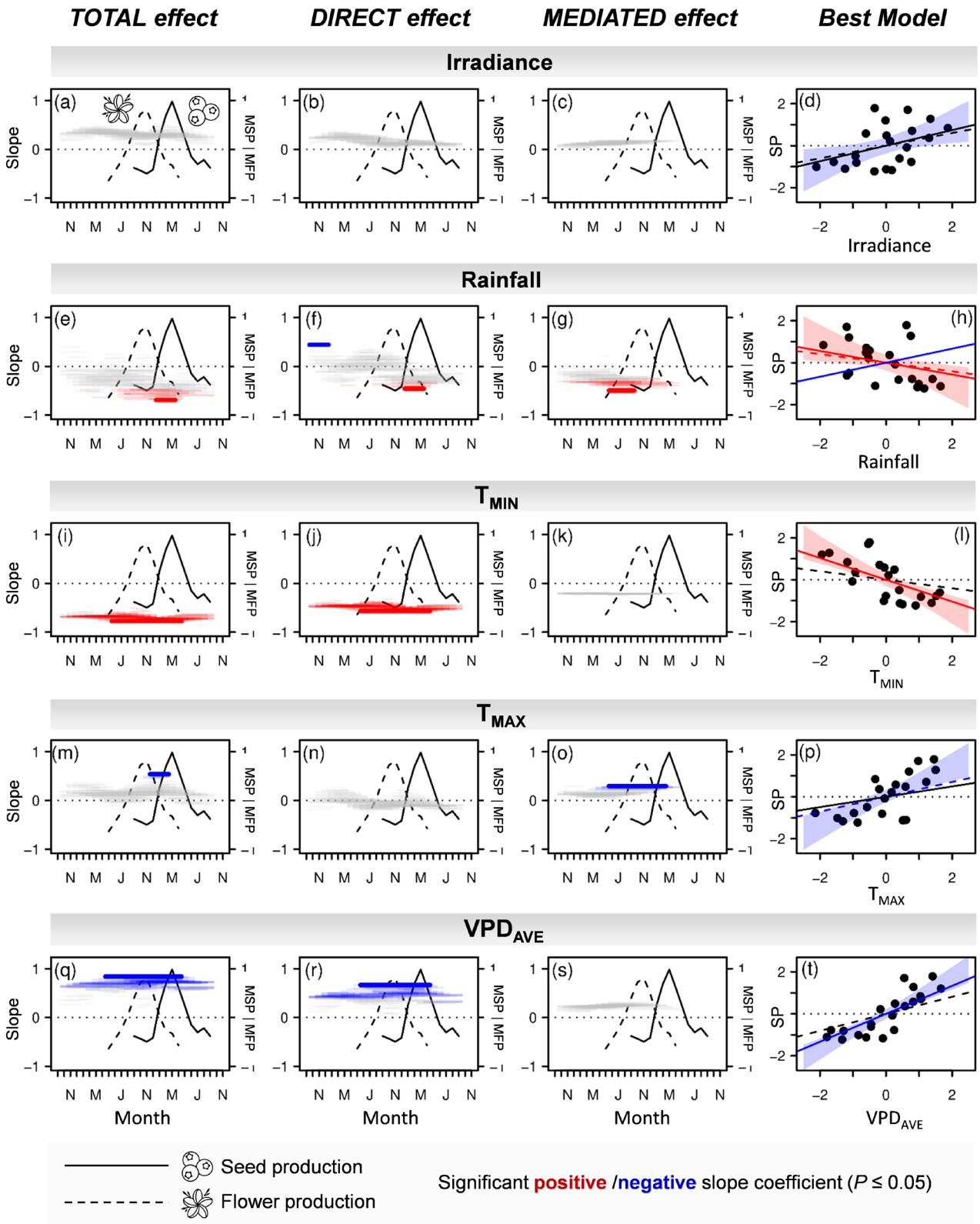

FIGURE 4 | Legend on next page.

addition to inducing light limitation, heavy cloud cover and rainfall could directly damage developing fruits or favour the proliferation of moisture-sensitive pests (Lebrija-Trejos, Hernández, and Wright 2023). The negative flower-mediated effect of mean rainfall during the onset of the flowering season (Figure 4g) may be explained by potential damage exerted by heavy rain on flowers, which in turn may result in reduced SP during the fruiting season.

The correlations between seed production and climate variables reported here are linear and mostly reflect long-term, decadal

FIGURE 4 | Slope coefficient values quantifying the effect (total, direct, flower-mediated) of each climate variable on seed production, and regression trends corresponding to these effects, following the steps indicated in Figure 2. The solid and dashed black lines in the three leftmost columns of graphs (a-c, e-g, i-k, m-o, q-s) represent the average monthly seed production and flower production over the 2000–2021 period (with values scaled between −1 and 1), as described in Figure 2b. In these graphs, the *X*-axis covers a 24-month period which spans the community-level flowering and fruiting phenological years. Only 3 months are indicated on the *X*-axis for clarity (N = November; M = March; J = July). On each of these graphs, blue, red and grey colours indicated if the slope coefficient of the effect (total, direct, mediated) of the climate variable on seed production was significantly positive, significantly negative and non-significant, respectively. The strongest significant positive/negative slope coefficients are emphasised with thicker blue/red horizontal bars. Each graph in the last column (d,h,l,p,t) shows the trend of the total (shaded confidence interval), direct (solid line) and flower-mediated (dashed line) effect of each climate variable (*X*-axis) on seed production (*Y*-axis), as shown in Figure 2c. The confidence interval of the total irradiance effect (panel d) is shaded in blue because 95% of slope values were positive in the Bayesian credibility interval, though no slope coefficients were significant with the MSR test.

trends. Correlations between seed production and climate may occur over temporal scales ranging from weeks to decades, possibly reflecting the influence of short-term climatic events or longer-term cycles inherent to the climate or plant community. A wavelet coherence analysis identified significant correlations at intermediate time scales (mostly from 32 to 64 months) for certain years (mostly between 2002 and 2012; Appendix S8, Figures S14–16). The wavelet coherence analyses also identified much stronger correlations between seed production and each climate variables at the annual scale and at the longest decadal scales that can be evaluated given 22 years of data (Appendix S8, Figures S14–16). Thus, the importance of long-term, decadal trends is confirmed.

4.4 | Comparison of Yasuní With Long-Term Pantropical Reproductive Phenology Studies

Long-term studies of tropical plant reproductive phenology have revealed diverse patterns across multiple time scales, partly influenced by the specific biogeographic and climatic context of each region (Morellato et al. 2016; Sullivan et al. 2023). The everwet forests of the Yasuní region have experienced relatively minor impacts from El Niño–Southern Oscillation (ENSO) events, in contrast to other tropical regions where ENSO likely plays a stronger role in driving reproductive cycles (Garwood et al. 2023). For instance, in Panama, a 30-year study showed a consistent rise in seed production following ENSO-driven increases in soil water deficit, vapour pressure deficit and solar irradiance, while no clear decadal trend was evident (Detto et al. 2018). Similarly, a 17-year study revealed no long-term fruiting trend in an everwet forest in Borneo but highlighted that supra-annual mast fruiting events were associated with temperature drops and drought periods, likely mediated by ENSO (Ushio et al. 2020). Lastly, ENSO significantly increased the number of flowering and fruiting species in an everwet forest at Luquillo, Puerto Rico, but reported effects were relatively weak and co-occurred with strong interannual variation which mirrored tree community recovery from hurricane disturbance (Zimmerman et al. 2018).

Long-term decadal shifts in fruit production have been reported in other regions. In Malaysian everwet forests, an increase in minimum temperature over 34 years was negatively correlated with fruit production, suggesting a disruption of cue-based reproductive processes (Numata et al. 2022). Thus, everwet forests in Malaysia and Ecuador show similar long-term declines in seed production, raising concerns that increasing nighttime temperatures may be progressively disrupting reproductive cycles in wetter areas of the tropics, even though such patterns are not generalisable to all everwet systems (Ushio et al. 2020). In contrast, patterns of increasing fruit production have been found in Africa. In two sites of tropical montane cloud forests in Uganda, Chapman et al. (2018) and Potts et al. (2020) found that interannual increase in irradiance, potentially mediated by ENSO, was associated with increased seed production over 15 and 19 years, respectively. Similarly, long-term increases in seed production have been reported in seasonal tropical forests in West Africa (Polansky and Boesch 2013) and Madagascar (Dunham et al. 2018), but these patterns were not clearly linked to any climate effects.

5 | Conclusion

Over 22 years of monitoring reproductive patterns in Yasuní's everwet tropical forest, we documented a decline in community-level seed production. This decline was primarily driven by increased nighttime temperatures and decreased water vapour pressure, although periods of higher daytime temperatures correlated with enhanced fruiting. Both positive and negative influences of rainfall on seed outputs were observed, depending on seasonal rain patterns. Continued long-term monitoring of flowering and fruiting cycles will be essential to track these shifts, which, if persisting in the coming decades, are likely to result in profound alterations in forest dynamics, with potential consequences for both forest structure and species composition.

Author Contributions

Jason Vleminckx, J. Aaron Hogan, Margaret R. Metz, Nancy C. Garwood, Simon A. Queenborough, Liza S. Comita, Renato Valencia and S. Joseph Wright contributed to the conception and/or design of the study. Nancy C. Garwood, S. Joseph Wright, Margaret R. Metz, Milton Zambrano, Simon A. Queenborough and Renato Valencia are involved in field data collection. Jason Vleminckx analysed the data with the help of J. Aaron Hogan, Liza S. Comita and S. Joseph Wright. Jason Vleminckx wrote the manuscript with the help of J. Aaron Hogan, Liza S. Comita, Simon A. Queenborough and S. Joseph Wright.

Acknowledgements

J.V. was funded by a G. Evelyn Hutchinson Environmental Postdoctoral Fellowship from the Yale Institute for Biospheric Studies (Yale University, CT, USA). We thank Pablo Alvia, Alvaro Pérez, Zornitza Aguilar, Paola

Barriga, Matt Priest, Caroline Whitefoord and Gorky Villa for assistance in collecting data or identifying species; Elina Gomez for entry of trap data; Hugo Navarrete, Katya Romoleroux and the QCA herbarium staff, and David Lasso and the ECY staff for help with logistics and needed permitting; Rick Condit, Elizabeth Losos, Robin Foster and Henrik Balslev for initial encouragement to work within the Yasuní Forest Dynamics Plot; Hugo Romero for initially summarising the YFDP and SSP weather data sets; Pablo Jarrin for setting up the TEAM weather station, and David Lasso and Carlos Padilla for maintaining that equipment and making the data available; and the Ecuadorian Ministerio del Ambiente for permission to work in Yasuní National Park. The Forest Dynamics Plot of Yasuní National Park has been made possible through the generous support of the Pontifical Catholic University of Ecuador (PUCE) funds of donaciones del impuesto a la renta, the government of Ecuador, the US National Science Foundation, the Andrew W. Mellon Foundation, the Smithsonian Tropical Research Institute and the University of Aarhus of Denmark. The project began while NCG was at the Natural History Museum, London, with funding (2000–2004) from the Department of Botany (NHM), the Andrew W. Mellon Foundation, British Airways and the Natural Environment Research Council (GR9/04037). It continued with NCG at Southern Illinois University Carbondale (2005–2021). We thank the Center for Tropical Forest Science for transitional funding (2006–2008, 2017–2018) and the National Science Foundation for long-term funding (2006–2020; DEB-0614525, DEB-1122634, DEB-1754632, DEB-1754668).

Data Availability Statement

The data supporting the results have been archived in a Dryad repository and can be accessed via the following URL: https://doi.org/10.5061/dryad.j9kd51ckz.

Peer Review

The peer review history for this article is available at https://www.webofscience.com/api/gateway/wos/peer-review/10.1111/ele.70019.

References

Abernethy, K., E. R. Bush, P.-M. Forget, I. Mendoza, and L. P. C. Morellato. 2018. "Current Issues in Tropical Phenology: A Synthesis." *Biotropica* 50: 477–482.

Aleixo, I., D. Norris, L. Hemerik, et al. 2019. "Amazonian Rainforest Tree Mortality Driven by Climate and Functional Traits." *Nature Climate Change* 9, no. 5: 384–388.

Atkin, O. K., D. Bruhn, V. M. Hurry, and M. G. Tjoelker. 2005. "Evans Review No. 2: The Hot and the Cold: Unravelling the Variable Response of Plant Respiration to Temperature." *Functional Plant Biology* 32, no. 2: 87–105.

Aun, M. A., F. Farnese, L. Loram-Lourenço, et al. 2024. "Evidence of Combined Flower Thermal and Drought Vulnerabilities Portends Reproductive Failure Under Hotter-Drought Conditions." *Plant, Cell & Environment* 47: 1971–1986.

Baraloto, C., J. Vleminckx, J. Engel, et al. 2021. "Biogeographic History and Habitat Specialization Shape Floristic and Phylogenetic Composition Across Amazonian Forests." *Ecological Monographs* 91, no. 4: e01473.

Bauman, D., C. Fortunel, L. A. Cernusak, et al. 2022. "Tropical Tree Growth Sensitivity to Climate Is Driven by Species Intrinsic Growth Rate and Leaf Traits." *Global Change Biology* 28, no. 4: 1414–1432.

Bauman, D., J. Vleminckx, O. J. Hardy, and T. Drouet. 2019. "Testing and Interpreting the Shared Space-Environment Fraction in Variation Partitioning Analyses of Ecological Data." *Oikos* 128, no. 2: 274–285.

Berdugo, M. B., L. Heyer, K. Y. S. Contento, et al. 2022. "High-Resolution Tropical Rain-Forest Canopy Climate Data." *Environmental Data Science* 1: e13.

Butt, N., L. Seabrook, M. Maron, et al. 2015. "Cascading Effects of Climate Extremes on Vertebrate Fauna Through Changes to Low-Latitude Tree Flowering and Fruiting Phenology." *Global Change Biology* 21, no. 9: 3267–3277.

Blanke, M. M., and F. Lenz. 1989. "Fruit Photosynthesis." *Plant, Cell & Environment* 12: 31–46.

Chapman, C. A., K. Valenta, T. R. Bonnell, K. A. Brown, and L. J. Chapman. 2018. "Solar Radiation and ENSO Predict Fruiting Phenology Patterns in a 15-Year Record From Kibale National Park, Uganda." *Biotropica* 50: 384–395.

Chen, Y. Y., A. Satake, I. F. Sun, et al. 2018. "Species-Specific Flowering Cues Among General Flowering Shorea Species at the Pasoh Research Forest, Malaysia." *Journal of Ecology* 106: 586–598.

Cleveland, R. B., W. S. Cleveland, J. E. McRae, and I. Terpenning. 1990. "STL: A Seasonal-Trend Decomposition Procedure Based on Loess." *Journal of Official Statistics* 6: 3–73.

Cook, B. I., E. M. Wolkovich, T. J. Davies, et al. 2012. "Sensitivity of Spring Phenology to Warming Across Temporal and Spatial Climate Gradients in Two Independent Databases." *Ecosystems* 15: 1283–1294.

Crous, K. Y., J. Uddling, and M. G. De Kauwe. 2022. "Temperature Responses of Photosynthesis and Respiration in Evergreen Trees From Boreal to Tropical Latitudes." *New Phytologist* 234: 353–374.

Davis, C. C., G. M. Lyra, D. S. Park, et al. 2022. "New Directions in Tropical Phenology." *Trends in Ecology & Evolution* 37, no. 8: 683–693.

Detto, M., S. J. Wright, O. Calderón, and H. C. Muller-Landau. 2018. "Resource Acquisition and Reproductive Strategies of Tropical Forest in Response to the El Niño–Southern Oscillation." *Nature Communications* 9, no. 1: 913.

Doughty, C. E., J. M. Keany, B. C. Wiebe, et al. 2023. "Tropical Forests Are Approaching Critical Temperature Thresholds." *Nature* 621, no. 7977: 105–111.

Dunham, A. E., O. H. Razafindratsima, P. Rakotonirina, and P. C. Wright. 2018. "Fruiting Phenology Is Linked to Rainfall Variability in a Tropical Rain Forest." *Biotropica* 50, no. 3: 396–404.

Fleischmann, A. S., F. Papa, S. K. Hamilton, et al. 2023. "Increased Floodplain Inundation in the Amazon Since 1980." *Environmental Research Letters* 18, no. 3: 034024.

Funatsu, B. M., R. Le Roux, D. Arvor, et al. 2021. "Assessing Precipitation Extremes (1981–2018) and Deep Convective Activity (2002–2018) in the Amazon Region With CHIRPS and AMSU Data." *Climate Dynamics* 57: 827–849.

Garwood, N. C., M. R. Metz, S. A. Queenborough, et al. 2023. "Seasonality of Reproduction in an Everwet Lowland Tropical Forest in Amazonian Ecuador." *Ecology* 104: e4133.

Gatti, L. V., L. S. Basso, J. B. Miller, et al. 2021. "Amazonia as a Carbon Source Linked to Deforestation and Climate Change." *Nature* 595, no. 7867: 388–393.

Grossiord, C., T. N. Buckley, L. A. Cernusak, et al. 2020. "Plant responses to rising vapor pressure deficit." *New Phytologist* 226: 1550–1566.

Hoorn, C., F. P. Wesselingh, H. ter Steege, et al. 2010. "Amazonia Through Time: Andean Uplift, Climate Change, Landscape Evolution, and Biodiversity." *Science* 330: 927–931.

Kullberg, A. T., L. Coombs, R. D. Soria Ahuanari, R. P. Fortier, and K. J. Feeley. 2024. "Leaf Thermal Safety Margins Decline at Hotter Temperatures in a Natural Warming 'experiment' in the Amazon." *New Phytologist* 241, no. 4: 1447–1463.

Lebrija-Trejos, E., A. Hernández, and S. J. Wright. 2023. "Effects of Moisture and Density-Dependent Interactions on Tropical Tree Diversity." *Nature* 615, no. 7950: 100–104.

Lin, H., Y. Chen, H. Zhang, P. Fu, and Z. Fan. 2017. "Stronger Cooling Effects of Transpiration and Leaf Physical Traits of Plants From a Hot Dry Habitat Than From a Hot Wet Habitat." *Functional Ecology* 31: 2202–2211.

Ljung, G. M., and G. E. P. Box. 1978. "On a Measure of Lack of Fit in Time Series Models." *Biometrika* 65, no. 2: 297–303.

Malo, G., and C. Arguello. 1984. *Proyecto Oriente, Mapa de Compilación Geológica de la Provincia Del Napo*. Quito, Eucador: Departamento de Geología, Instituto Ecuatoriano de Minería, Ministerio de Energía y Minas.

McGregor, G. R., and S. Niewold. 1998. *Tropical Climatology: An Introduction to the Climates of the Low Latitudes*. 2nd ed, 352. Chichester, UK: John Wiley & Sons.

Mendoza, I., C. A. Peres, and L. P. C. Morellato. 2017. "Continental-Scale Patterns and Climatic Drivers of Fruiting Phenology: A Quantitative Neotropical Review." *Global and Planetary Change* 148: 227–241.

Min, Q. 2004. "Retrievals of Thin Cloud Optical Depth From a Multifilter Rotating Shadowband Radiometer." *Journal of Geophysical Research* 109: 1–10.

Mitchard, E. T. A. 2018. "The Tropical Forest Carbon Cycle and Climate Change." *Nature* 559: 527–534.

Morellato, L. P. C., B. Alberton, S. T. Alvarado, et al. 2016. "Linking Plant Phenology to Conservation Biology." *Biological Conservation* 195: 60–72.

Numata, S., K. Yamaguchi, M. Shimizu, et al. 2022. "Impacts of Climate Change on Reproductive Phenology in Tropical Rainforests of Southeast Asia." *Communications Biology* 5: 311.

Ometto, J. P., K. Kalaba, G. Z. Anshari, et al. 2022. "CrossChapter Paper 7: Tropical Forests." In *Climate Change 2022: Impacts, Adaptation and Vulnerability. Contribution of Working Group II to the Sixth Assessment Report of the Intergovernmental Panel on Climate Change*, edited by H.-O. Pörtner, D. C. Roberts, M. Tignor, E. S. Poloczanska, K. Mintenbeck, A. Alegría, M. Craig, S. Langsdorf, S. Löschke, V. Möller, A. Okem, and B. Rama, 2369–2410. Cambridge, UK and New York, NY, USA: Cambridge University Press.

Pan, Y., R. A. Birdsey, J. Fang, et al. 2011. "A Large and Persistent Carbon Sink in the World's Forests." *Science* 333, no. 6045: 988–993.

Parsons, L. A. 2020. "Implications of CMIP6 Projected Drying Trends for 21st Century Amazonian Drought Risk." *Earth's Futures* 8: e2020EF001608.

Pau, S., D. K. Okamoto, O. Calderón, and S. J. Wright. 2018. "Long-Term Increases in Tropical Flowering Activity Across Growth Forms in Response to Rising CO_2 and Climate Change." *Global Change Biology* 24, no. 5: 2105–2116.

Pau, S., E. Wolkovich, B. Cook, et al. 2013. "Clouds and Temperature Drive Dynamic Changes in Tropical Flower Production." *Nature Climate Change* 3: 838–842.

Perez, T. M., and K. J. Feeley. 2018. "Increasing Humidity Threatens Tropical Rainforests." *Frontiers in Ecology and Evolution* 6: 68.

Pitman, N. C. A. 2000. *A Large-Scale Inventory of Two Amazonian Tree Communities*. PhD: Duke University.

Polansky, L., and C. Boesch. 2013. "Long-Term Changes in Fruit Phenology in a West African Lowland Tropical Rain Forest Are Not Explained by Rainfall." *Biotropica* 45, no. 4: 434–440.

Potts, K. B., D. P. Watts, K. E. Langergraber, and J. C. Mitani. 2020. "Long-Term Trends in Fruit Production in a Tropical Forest at Ngogo, Kibale National Park, Uganda." *Biotropica* 52: 521–532.

Queenborough, S. A., D. F. Burslem, N. C. Garwood, and R. Valencia. 2007. "Habitat Niche Partitioning by 16 Species of Myristicaceae in Amazonian Ecuador." *Plant Ecology* 192: 193–207.

R Core Team. 2024. "R: A Language and Environment for Statistical Computing." R Foundation for Statistical Computing, Vienna, Austria. https://www.R-project.org/.

Rodwell, L., K. J. Lee, H. Romaniuk, and J. B. Carlin. 2014. "Comparison of Methods for Imputing Limited-Range Variables: A Simulation Study." *BMC Medical Research Methodology* 14: 1–11.

Schrodt, F., J. Kattge, H. Shan, et al. 2015. "BHPMF – A Hierarchical Bayesian Approach to Gap-Filling and Trait Prediction for Macroecology and Functional Biogeography." *Global Ecology and Biogeography* 24: 1510–1521.

Slik, J. F., V. Arroyo-Rodríguez, S. I. Aiba, et al. 2015. "An Estimate of the Number of Tropical Tree Species." *Proceedings of the National Academy of Sciences* 112, no. 24: 7472–7477.

Slot, M., C. Rey-Sánchez, S. Gerber, J. W. Lichstein, K. Winter, and K. Kitajima. 2014. "Thermal Acclimation of Leaf Respiration of Tropical Trees and Lianas: Response to Experimental Canopy Warming, and Consequences for Tropical Forest Carbon Balance." *Global Change Biology* 20: 2915–2926.

Slot, M., and K. Winter. 2017. "In Situ Temperature Response of Photosynthesis of 42 Tree and Liana Species in the Canopy of Two Panamanian Lowland Tropical Forests With Contrasting Rainfall Regimes." *New Phytologist* 214: 1103–1117.

Sullivan, M. J. P., S. L. Lewis, K. Affum-Baffoe, et al. 2020. "Long-Term Thermal Sensitivity of Earth's Tropical Forests." *Science* 368: 869–874.

Sullivan, M. K., A. Fayolle, E. Bush, et al. 2023. "Cascading Effects of Climate Change: New Advances in Drivers and Shifts of Tropical Reproductive Phenology." *Plant Ecology* 225, no. 3: 175–187.

Tetens, O. 1930. "Uber Einige Meteorologische Begriffe." *Zeitschrift für Geophysik* 6: 297–309.

Tibbitts, T. W. 1979. "Humidity and Plants." *Bioscience* 29: 358–363.

Tutin, C. E. G., and M. Fernandez. 1993. "Relationships Between Minimum Temperature and Fruit Production in Some Tropical Forest Trees in Gabon." *Journal of Tropical Ecology* 9: 241–248.

Ushio, M., Y. Osada, T. O. Kumagai, et al. 2020. "Dynamic and Synergistic Influences of Air Temperature and Rainfall on General Flowering in a Bornean Lowland Tropical Forest." *Ecological Research* 35, no. 1: 17–29.

Valencia, R., R. S. Condit, K. Romoleroux, et al. 2004. "Yasuní Forest Dynamics Plot, Ecuador." In *Tropical Forest Diversity and Dynamism: Findings From a Large-Scale Plot Network*, edited by E. C. Losos and E. G. J. Leigh, 609–620. Chicago, IL: University of Chicago Press.

Valencia, R., R. B. Foster, G. Villa, et al. 2004. "Tree Species Distributions and Local Habitat Variation in the Amazon: Large Forest Plot in Eastern Ecuador." *Journal of Ecology* 92: 214–229.

Van Schaik, C. P., J. W. Terborgh, and S. J. Wright. 1993. "The Phenology of Tropical Forests: Adaptive Significance and Consequences for Primary Consumers." *Annual Review of Ecology and Systematics* 24, no. 1: 353–377.

Vleminckx, J., J. A. Hogan, M. R. Metz, et al. 2023. "Flower Production Decreases With Warmer and More Humid Atmospheric Conditions in a Western Amazonian Forest." *New Phytologist* 241, no. 3: 1035–1046.

Walter, H., E. Harnickell, and D. Mueller-Dombois. 1975. *Climate-Diagram Maps of the Ecological Regions of the Earth*, 36. Berlin, Germany: Springer.

Wagner, H. H., and S. Dray. 2015. "Generating Spatially Constrained Null Models for Irregularly Spaced Data Using Moran Spectral Randomization Methods." *Methods in Ecology and Evolution* 6, no. 10: 1169–1178.

Williamson, G. B., W. F. Laurance, A. A. Oliveira, et al. 2000. "Amazonian Tree Mortality During the 1997 El Nino Drought." *Conservation Biology* 14, no. 5: 1538–1542.

Windsor, D. M. 1990. "Climate and Moisture Variability in a Tropical Forest: Long-Term Records for Barro Colorado Island, Panama." *Smithsonian Contributions to the Earth Sciences* 29: 1–145.

Wright, S. J., and O. Calderon. 1995. "Phylogenetic Patterns Among Tropical Flowering Phenologies." *Journal of Ecology* 83: 937–948.

Wright, S. J., and O. Calderon. 2006. "Seasonal, El Niño and Longer Term Changes in Flower and Seed Production in a Moist Tropical Forest." *Ecology Letters* 9: 35–44.

Wright, S. J., and O. Calderon. 2018. "Solar Irradiance as the Proximate Cue for Flowering in a Tropical Moist Forest." *Biotropica* 50, no. 3: 374–383.

Wright, S. J., and C. P. Van Schaik. 1994. "Light and the Phenology of Tropical Trees." *American Naturalist* 143, no. 1: 192–199.

Zimmerman, J. K., J. A. Hogan, C. J. Nytch, and J. E. Bithorn. 2018. "Effects of Hurricanes and Climate Oscillations on Annual Variation in Reproduction in Wet Forest, Puerto Rico." *Ecology* 99, no. 6: 1402–1410.

Supporting Information

Additional supporting information can be found online in the Supporting Information section.